Heliyon 10 (2024) e37290

Contents lists available at ScienceDirect

Heliyon

journal homepage: www.cell.com/heliyon

Research article

Prognostic signature and immune landscape of 5-methylcytosine-related long non-coding RNAs in gastric cancer

Qingyu Song [a,1], Jingyu Wu [b,1], Hao Wan [c], Desen Fan [d,*]

[a] Department of General Surgery, The Second Affiliated Hospital of Nanjing Medical University, Nanjing, China
[b] Department of General Surgery, The First Affiliated Hospital of Nanjing Medical University, Nanjing, China
[c] Department of Environmental Genomics, Jiangsu Key Laboratory of Cancer Biomarkers, Prevention and Treatment, Collaborative Innovation Center for Cancer Personalized Medicine, School of Public Health, Nanjing Medical University, Nanjing, 211166, China
[d] The Affiliated Jiangning Hospital with Nanjing Medical University, Nanjing, Jiangsu, 211100, China

ARTICLE INFO

Keywords:
m5C-lncRNAs
Gastric cancer
Signature
Nomogram
The tumor immune microenvironment

ABSTRACT

Background: Long non-coding RNAs (lncRNAs) have been demonstrated to be useful in assessing the prognosis of cancer patients. However, few studies have focused on 5-methylcytosine-related lncRNAs (m5C-lncRNAs) in gastric cancer (GC). In this study, we aimed to establish a m5C-lncRNAs prognostic signature (m5C-LPS) and explore its potential impact on guiding clinical practice for GC.

Methods: RNA-sequence and clinicopathological data were retrieved from The Cancer Genome Atlas (TCGA) database, while the coexpression of long non-coding RNAs (lncRNAs) was determined using Pearson's correlation analysis. A m5C-LPS model was constructed using univariate and Lasso Cox regression, and its prognostic value and accuracy were subsequently validated. Subsequently, the expression of 11 m5C-lncRNAs was verified via quantitative real-time PCR (qRT-PCR) in gastric cancer (GC) cell lines. The potential biological mechanism of this signature was elucidated using Gene Set Enrichment Analysis (GSEA). Based on the GSEA findings, CIBERSORT and ESTIMATE algorithms were utilized to conduct a comprehensive investigation of the tumor immune microenvironment (TIME) in GC. Additionally, pRRophetic and TIDE algorithms were employed to predict drug sensitivity and the efficacy of immunotherapy for GC patients.

Results: 280 lncRNAs were identified as m5C-lncRNAs, including RHPN1-AS1, AC093752.3, TSC22D1-AS1, AL391152.1, MAGI2-AS3, AC048382.2, AL033527.3, AC007405.2, AC036103.1, CCDC183-AS1, and ADORA2A-AS1. Their prognostic value was validated, and the expression of these 11 lncRNAs was confirmed in four gastric cancer cell lines using quantitative reverse transcription PCR (qRT-PCR). A nomogram incorporating a risk score was developed to provide more precise clinical decision-making. Gene Set Enrichment Analysis (GSEA) showed that many classical signaling pathways related to tumor progression were enriched in this signature. Analyses related to immunity and drug sensitivity demonstrated distinct differences in features between high-risk and low-risk subgroups.

Conclusion: The m5C-LPS can predict the survival of gastric cancer (GC) patients, provide novel therapeutic targets, and thus offer more thoughtful perspectives for future clinical decisions regarding GC.

* Corresponding author.
E-mail address: 13814063835@163.com (D. Fan).
[1] Song Qingyu and Wu Jingyu are co-first authors and contribute equally to the article.

https://doi.org/10.1016/j.heliyon.2024.e37290
Received 25 August 2023; Received in revised form 27 August 2024; Accepted 30 August 2024
Available online 14 September 2024

1. Introduction

Gastric cancer (GC) is a prevalent malignancy worldwide, in 2020, there were roughly 1,089,103 new cases (5.6 %) and 768,793 new deaths (7.7 %), placing the fifth in morbidity and the fourth in mortality [1]. Despite the detection, diagnosis and treatment of GC have obtained significant developments in recent years, the survival rate of GC remains unsatisfactory owing to absence of early specific symptoms and tendency to postoperative recurrence [2]. In recent years, targeted therapy and immune checkpoint inhibitors have made effective improvements for patients with GC. Yet, the high rate of immunotherapy resistance remains a noteworthy issue. Therefore, developing a novel biomarker seems essential for the prognostic prediction and clinical treatment. Prognostic ModelsBy comparing the effects of different treatments, new prognostic models can help us choose the best treatment options, thereby improving the quality of life and survival of patients [3].

RNA methylation, plays a crucial role in epigenetics and is closely related to many human diseases, including cancer, immune disorders and neurological diseases [4]. 5-methylcytosine (m5C), catalyzing its target genes by methylating the fifth carbon of cytosine, is a common mRNA methylation modification form [5]. The whole process is catalyzed by three enzymes, named methyltransferase ("writer"), demethylase ("Eraser"), as well as binding protein ("Reader"). m5C was proved essential in the development of tumor cells, such as RNA splicing, translation, degradation and protein processing. Chen X et al. found, in bladder cancer, YBX1, which is a reader protein, could bind to the 3′UTR of target genes and recruit ELAVL1 to maintain the stability of its identified genes to further affect cancer progression [6].Besides, in numerous studies, the expression of m5C-related genes have been verified closely related to the prognosis of malignant tumors, as well as vital in regulating tumor growth and directing clinical managements [7–9].

Long non-coding RNA (lncRNAs), with length over 200 nucleotides, are known to be critical in regulating gene expression in numerous diseases [10]. The abnormal expression of lncRNAs could make significant influence on tumor cells proliferation, invasion and apoptosis, thus affecting the occurrence, development and prognosis of cancer patients [11–13]. Methylation-related genes could regulate the methylation level of lncRNAs to influence the progression of tumor. For instance, Sun Z et al. discovered that lncRNA H19, which was modified by NSUN2, could promote the progress of liver cancer via recruiting the G3BP1 oncoprotein [14]. In colorectal cancer, lncRNA LINRIS was proved could reduce the ubiquitination of the m6A "reader" IGF2BP2 to promote the tumor development and the aerobic glycolysis [15]. Furthermore, m5C-related lncRNAs (m5C-lncRNAs) have been utilized in numerous cancers to construct a signature and forecast their survival status [16–18]. Nevertheless, the functions of m5C-lncRNAs in GC remain a mystery. Hence, it is extremely significant to develop a m5C-lncRNAs prognostic signature (m5C-LPS) and probe their potential role in the development of GC. The tumor microenvironment (TME), encompassing immune cells, stromal cells, extracellular matrix, secreted molecules, and vascular networks, interacts with cancer cells [19,20]. The tumor immune microenvironment (TIME) influences tumor evolution and therapeutic responses, as immune cells initially target cancer cells, which often develop resistance [21]. LncRNAs play a significant role in modulating TIME. While their relationship with TIME has been established in diverse cancers [22–24], further investigation is warranted to discern their association with m5C-lncRNAs in GC.

In our study, we identified and constructed an 11-gene m5C-LPS for GC using bioinformatics approaches. We validated its prognostic efficacy, assessed potential correlations between TIME components and m5C-LPS, examined the immunotherapy response, and identified potential therapeutic agents for GC.

2. Materials and methods

2.1. Data collection

Transcriptome data (FPKM format) and clinicopathology data up to January 2022 were downloaded from TCGA Platform (https://portal.gdc.cancer.gov/). We obtained 343 GC tissues and 30 normal tissues gene expression data and clinicopathology data of 443 GC patients based on Strawberry Perl tool. Table S1 lists clinical characteristics of the 443 patients with gastric cancer.

2.2. Identification of m5C-lncRNAs

19 m5C regulators (writers: NSUN1, NSUN2, NSUN3, NSUN4, NSUN5, NSUN6, NSUN7, DNMT2, DNMT3A, DNMT3B, NOL1, NOP2; erasers: TET2, ALKBH1, TET1, TET3; readers: ALYREF, YBX1) were obtained based on previous issued articles [25–27]. 13162 lncRNAs were identified in TCGA GC cohort according to the lncRNAs annotation file of the GENCODE website (https://www.gencodegenes.org/). We constructed a coexpression network between lncRNAs and 19 m5C regulators to identify the m5C-lncRNAs by the utilization of R program with "limma" package ($|\text{Pearson } R| > 0.4$ and $P < 0.001$).

2.3. Construction of m5C-LPS

Univariate cox regression was utilized via the "survival" package to obtain lncRNAs of prognostic value ($P < 0.05$). Then patients in TCGA database were split into two datasets randomly: the train dataset and the test dataset. we further performed the Lasso cox regression in the train dataset to construct a m5C-LPS. Then, each sample's risk score could be estimated by the following equation:

$$Risk\ score = \sum_{i=1}^{n} (Coef(i) \times Exp(i)),$$

where coef(i) refers to the survival correlation coefficient and Exp(i) refers to the expression of each m5C-lncRNAs, respectively.

2.4. Assessment of the prognostic signature and establishment of the nomogram

The median prognostic value of the train dataset was calculated as cut-off, and the train and test GC datasets were next split into high- and low-risk subgroups respectively. Receiver operating characteristics (ROC) curves, Principal component analysis (PCA) as well as the Kaplan-Meier (KM) survival curves were adopted in order to valid the prediction accuracy and prognostic value of this signature and reduce dimension. Univariate and multivariate cox regression were conducted to determine factors that could be independently used to assess the prognosis ($P < 0.05$). The nomogram was established based on age, stage and risk score. Meanwhile, whether the predicted results are in favorable consistence with the actual results was verified by calibration curves.

2.5. Gene Set Enrichment Analysis (GSEA)

In order to probe which signaling pathways the signature might be involved in. We calculated the differential genes between the two subgroups and next performed GSEA in the entire GC cohort, with the clusterProfiler package ($P < 0.05$).

2.6. Analysis of TIME

According to the results of GSEA, we decided to investigate the role of TIME in the progression of GC. The infiltration status of 22 immune cells were calculated via the CIBERSORT package in each sample. Then, the difference of 22 infiltrated immune cells, immune functions as well as immune checkpoints between subgroups were detected. The correlation between 22 immune cells and risk score was later calculated by 7 platforms algorithms including XCELL, TIMER, etc. The estimate and limma packages were performed to compare the immunescore, stromalscore, and estimatescore between the risk subgroups to analyze the TIME.

2.7. Application in clinical treatment

The pRRophetic package was used to assess the drug sensitivity between the subgroups according to the half-maximal inhibitory concentration (IC50) in GC patients. And as a result, sensitive drugs were obtained and might become candidates for different populations' treatment. Furthermore, Tumor Immune Dysfunction and Exclusion (TIDE) algorithm was utilized to determine whether the GC population could benefit from immunotherapy. TIDE (http://tide.dfci.harvard.edu/) stands for Tumour Immune Dysfunction and Exclusion. This computational framework is employed to evaluate the potential of tumour immune evasion based on the gene expression profiles of tumour samples. The TIDE score, computed for each tumour sample, can act as an alternative biomarker, predicting the response to immune checkpoint blockade.

2.8. Cell lines and reagents

Human normal gastric mucosal cells GES-1 and gastric cancer cell lines AGS, HGC-27, SGC-7901 were obtained from the type Culture Collection of the Chinese Academy of Sciences (Shanghai, China). All cells were cultured in RPMI 1640 median (VivaCell, shanghai, China) containing 10 % fetal bovine serum (VivaCell, shanghai, China), and all cells were cultured in incubator at 37 °C and 5 % CO_2.

2.9. RNA extration and qRT-PCR

We extracted total RNA from GC cell lines with TRIzol reagent (Invitrogen, USA). Then, RNA was synthesized into cDNA by using HiScript II (Vazyme, China). The following PCR procedures were used, using the Roche 480 fluorescence quantitative PCR instrument as an example: a. Reverse transcription:50 °C 15~30mins. pre-denaturation: 95 °C 2mins. denaturation: 95 °C 15secd. annealing/extension: 60 °C 15~30secs. Repeat step C and step D for a total of 40 cycles. The results of the three-step method were analyzed using the software provided with the PCR instrument. GAPDH was applied as the internal reference. The primers used for qRT-PCR were listed in Table S2.

2.10. Research objectives

Our primary objective is the establishment of the m5C-LPS model. Subsequently, we evaluate the prognostic significance of m5C-LPS for gastric cancer patients by conducting Gene Set Enrichment Analysis (GSEA), tumor microenvironment assessment, immunochemotherapy response evaluation, and drug prediction studies. Finally, we confirm the efficacy of m5C-LPS across various cohorts and ascertain its precision using nomogram curves.

2.11. Statistical analysis

Pearson analysis was used to compute correlation correlation (cor >0.04). The KM survival curves, Cox regression model were utilized to assess the prognostic value of the signature. GSEA was used for functional annotation. One-way ANOVA was applied to analyze the results of RT-qPCR. $P < 0.05$ was considered statistically significant.

3. Results

3.1. Identification of m5C-lncRNAs in GC

Flowchart of current research was exhibited in Fig. 1. 13162 lncRNAs and 19 m5C regulators expression data were obtained from TCGA transcriptomic data. Next, we performed coexpression analysis between 19 regulators and lncRNAs, and as a result, 280 lncRNAs were identify the m5C-lncRNAs. The coexpression network plot was shown in Fig. 2A. Moreover, we conducted a univariate cox regression, as a result, 11 lncRNAs with prognostic value were obtained and visualized as a forest plot in Fig. 2B ($P < 0.05$). Then, the differential expression levels of 11 prognosis-related lncRNAs between neoplasm and adjacent normal tissues were showed in heatmaps and boxplots (Fig. 2C and D).

3.2. Establishment of 11 m5C-LPS for GC populations

For developing a gene signature associated with m5C-lncRNAs to predict GC prognosis, we divided 338 GC samples into two datasets: a train dataset (N = 170) and a test dataset (N = 168). Then the train dataset was randomly performed Lasso cox regression. As a result, 11 m5C-lncRNAs were identified and we constructed a 11-gene prognostic signature (Fig. 3A and B). The risk score for the entire cohort could be calculated by the below equation: risk score = RHPN1-AS1 × 0.0286750810771526 + AC093752.3 × (−0.370108723776425) + TSC22D1-AS1 × (−0.871765391370144) + AL391152.1 × 0.360518383302827 + MAGI2-AS3 × 0.211794421769072 + AC048382.2 × 1.02071894349808 + AL033527.3 × (−1.39673260675422) + AC007405.2 × (−0.522255103119796) + AC036103.1 × 0.689804086658695 + CCDC183-AS1 × (−0.0500150604730576) + ADORA2A-AS1 × 0.134675382468313. The Sankey plot revealed the regulatory relationships between the 9 m5C regulators and 11 selected lncRNAs (Fig. 3C). The PCA showed that GC patients can be well separated into two significantly different subgroups (Fig. 3D). Moreover, the area under the curve (AUC) for 1, 3, 5-year OS was 0.709, 0.731, 0.771 in the entire dataset. As shown in the 1-year ROC curve, the AUC of risk score (0.709) exhibited superior to the conventional clinical factors such as age (0.594), gender (0.525), grade (0.562) and stage (0.603). The results implied that the m5C-LPS had an excellent sensitivity and accuracy in forecasting the prognosis of GC (Fig. 3E and F).

3.3. Prognostic value assessment of the signature

KM curves revealed the low-risk subgroup survived much better both in the train and test datasets ($P < 0.05$) (Fig. 4A and B). We ranked the GC samples in order by the risk score, and further attempted to analyze the expression level, the risk score distribution as well as the survival status. Heatmap depicted the relative differential expression level of 11 m5C-lncRNAs between the subgroups (Fig. 4C and D). Moreover, the scatter dot diagram revealed, as the risk score increased, more GC patients would be correspondingly exhibited dead, meanwhile, patients with high scores displayed a greater tendency to have shorter survival time (Fig. 4E–H). As the risk score increases, the prognosis for gastric cancer patients deteriorates irrespective of age, gender, and tumor stage. (Supplementary

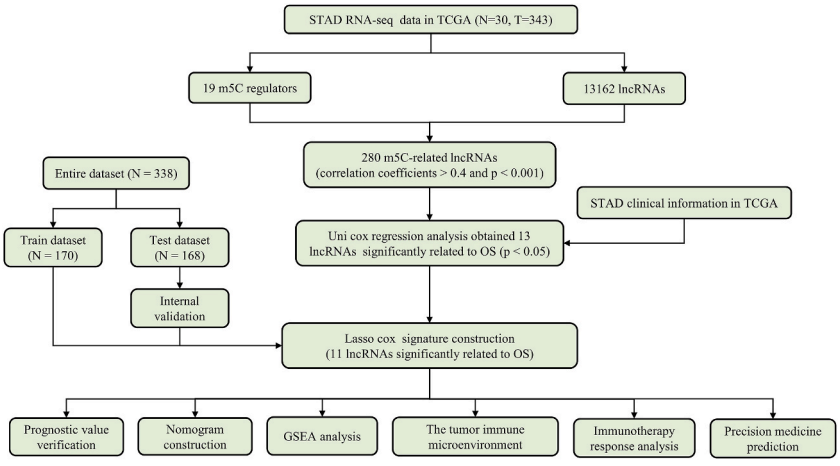

Fig. 1. The flowchart of current research.

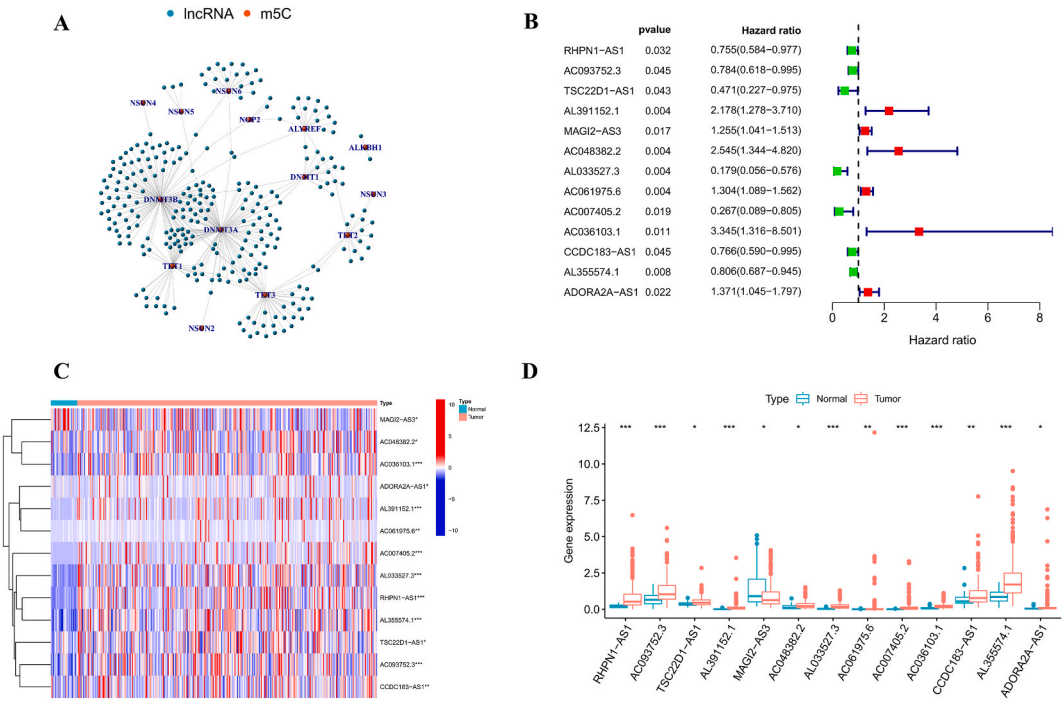

Fig. 2. Identification of prognostic m5C-lncRNAs in GC. (A) The coexpression network of 280 m5C-lncRNAs and 19 m5C regulators in GC. (B) The forest plot of 11 prognostic lncRNAs obtained by univariate cox analysis. (C–D) The differential expression of 11 lncRNAs in tumor and adjacent normal tissues of GC patients. $*P < 0.05$, $**P < 0.01$, $***P < 0.001$.

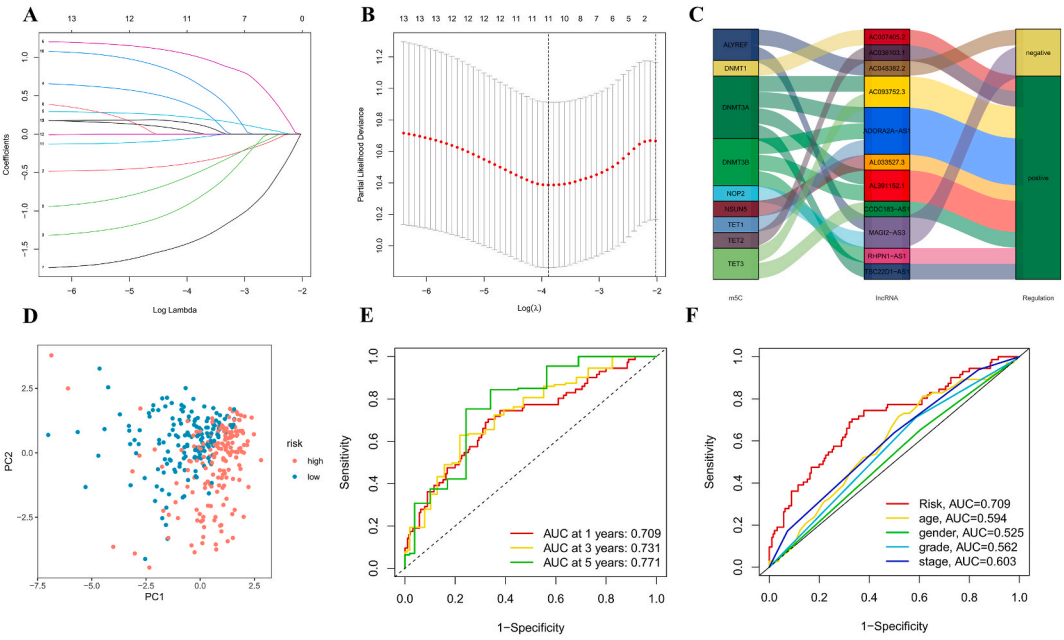

Fig. 3. Construction of 11 m5C-LPS in the GC. (A, B) Lasso cox regression and Cross-validation used to signature construction. (C) The relationship between the 9 m5C regulators and 11 m5C-lncRNAs. (D) PCA analysis based on the entire cohort between the subgroups. (E) ROC curves of the risk score in predicting 1-, 3-, 5-year OS. (F) ROC curves of the risk score and conventional clinicopathological factors for predicting 1-year OS.

Fig. S1). Univariate and multivariate cox regression demonstrated the risk score estimated by the signature could be independent from other clinicopathological factors, additionally, clinical factors such as age and stage also had the same effect, and these three indicators could be applied to establish a nomogram to assist clinical assessment (Fig. 5A–D).

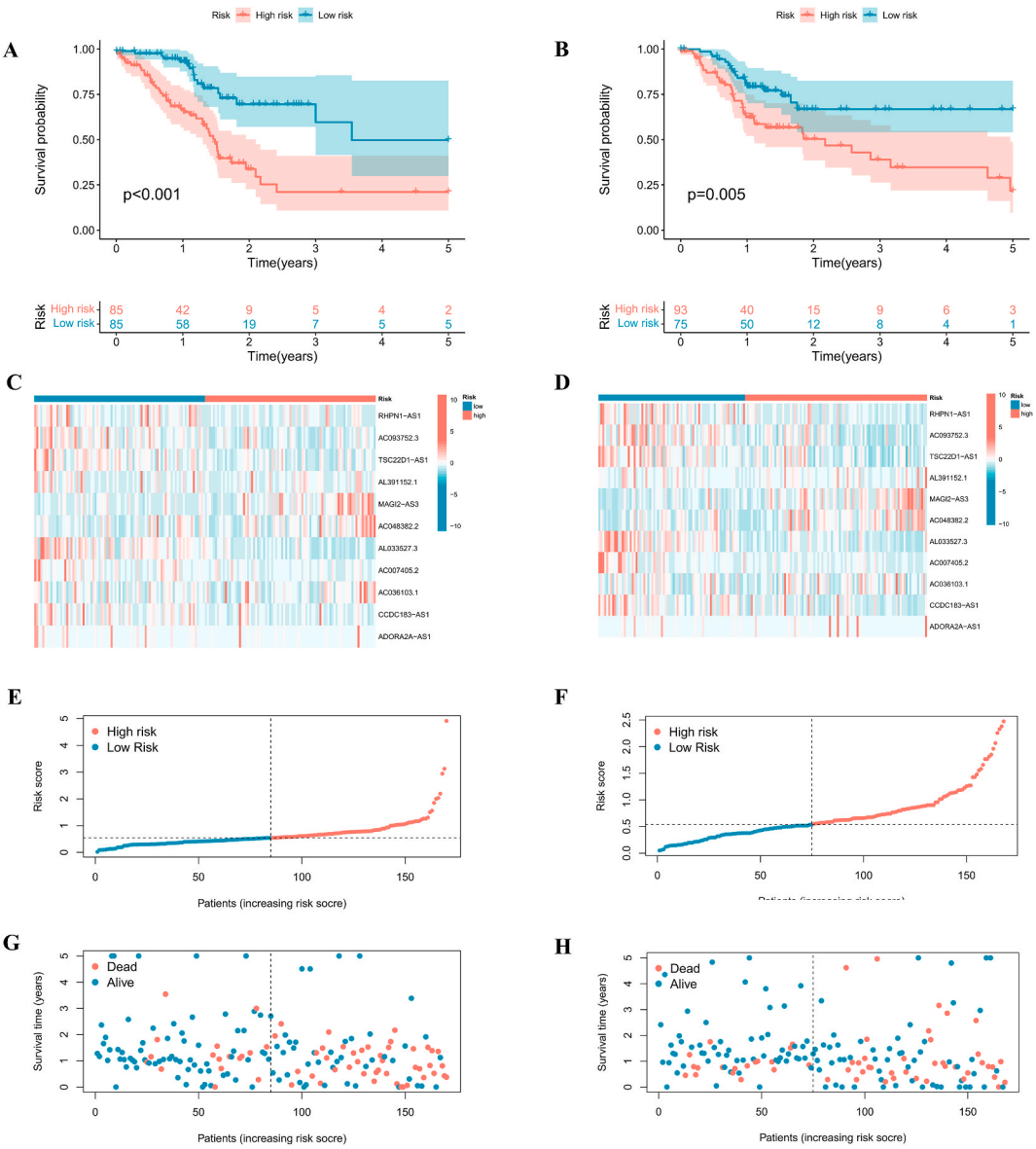

Fig. 4. Prognosis value validation of 11 m5C-lncRNAs in the train and test datasets. (A, B) KM curves of OS (C, D) and differential expression of 11 lncRNAs between two subgroups. (E–H) Risk score distribution and survival status of each patient in the train and test datasets. (the left is the train dataset and the right is the test dataset).

3.4. Construction of the nomogram

To make accurate forecast of the GC patients OS, age, stage as well as risk score were employed and estimated for the nomogram establishment. With the help of nomogram, we could better anticipate the 1-, 3-, 5-year OS (Fig. 5E). And the 1-, 3-, 5-year calibration plots verified the nomogram was of excellent predictive value and accuracy (Fig. 5F).

3.5. Gene Set Enrichment Analysis

To identify the potential effects m5C-lncRNAs might exert, GSEA was carried out. And as a result, massive classic cancer-related signaling pathways were enriched. Wnt, calcium, TGF-β, PI3K-Akt and Hedgehog signaling pathway, gastric cancer, complement and coagulation cascades were considered markedly related to the two subgroups ($P < 0.05$) (Fig. 6A and B). Some of these pathways were verified to be involved in immune infiltration and immune-related therapy [28,29]. Therefore, we attempted to perform analysis of immunity on the signature.

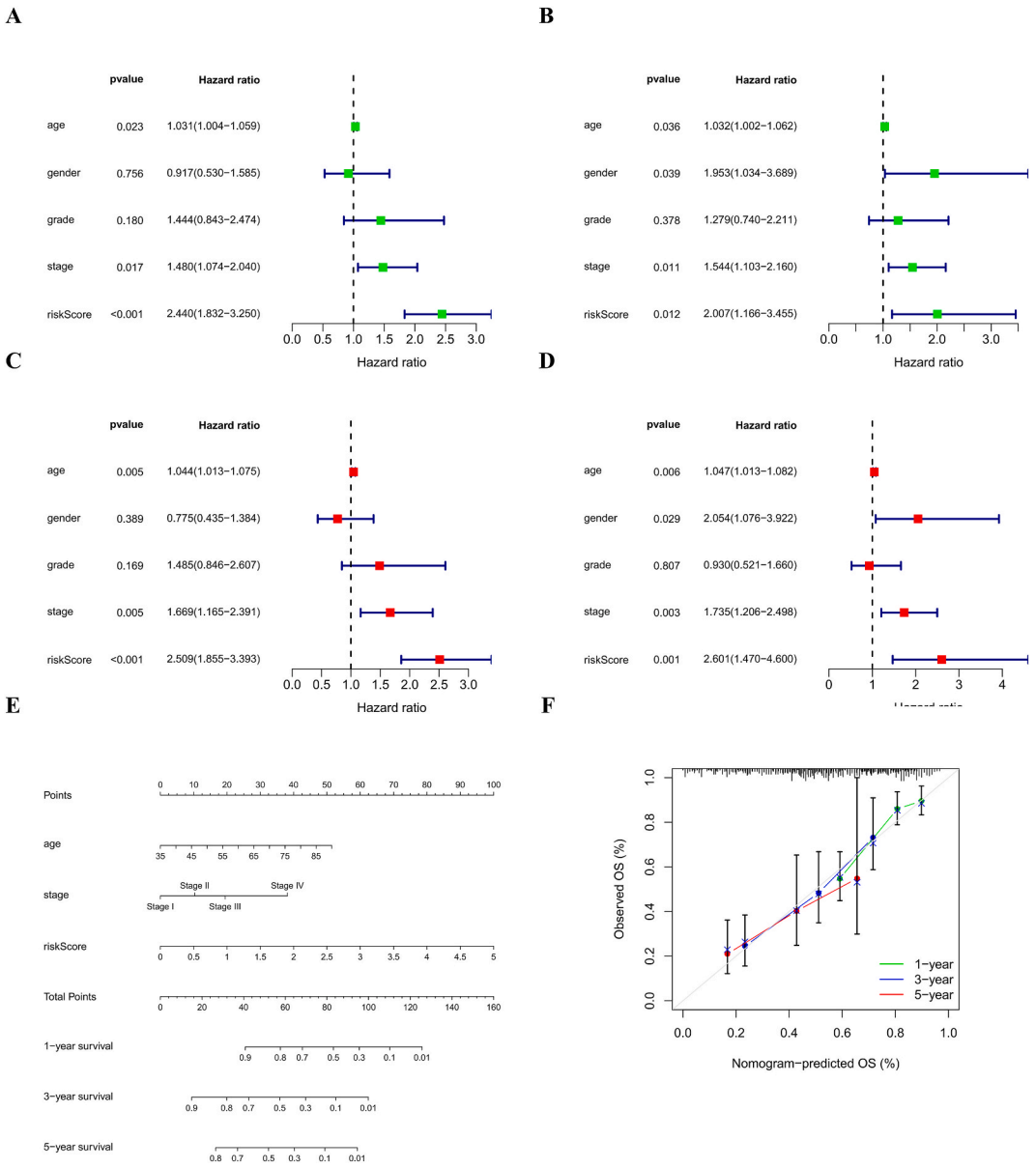

Fig. 5. Identification of independent prognostic indicators and construction of a nomogram. (A–B) Univariate cox regression in the train and test datasets. (C–D) Multivariate cox regression in the train and test datasets. (the left is the train dataset and the right is the test dataset). (E) The nomogram established on the basis of independent prognostic predictors for clinical anticipation. (F) The calibration curves.

3.6. The role of TIME in GC

To explore the role of immune infiltration in this signature, a series of immune-related analysis were performed. As shown in Fig. 7A, the expression of 22 immune cells differed prominently between the subgroups. T cells follicular helper, Macrophages M0, NK cells resting demonstrated a relative elevated content in the low-risk subgroup. However, at the same time, Monocytes, Macrophages M2, Dendritic cells resting and Mast cells resting were observed to have a moderately higher content in the high-risk subgroup ($P <$ 0.05). Moreover, in terms of immune functions, significant differences existed between the subgroups such as CCR, checkpoint, HLA, MHC-I, etc. (Fig. 7B). Similarly, the content of immune checkpoints existed differences, such as CD86, LAIR1, CD27, BTLA, etc. (Fig. 7C). Bubble chart exhibited the majority of immune cells infiltrated, which were estimated by 7 different platforms algorithms, tended to be positively correlated with the risk score (Fig. 7D). What's more, we also found that 5 immune-infiltrating cells (Dendritic cells resting, Monocytes, Macrophages M2, Mast cells resting, T cells CD4 memory resting) tended to express more as the risk score increased, but 3 immune cells (NK cells resting, Macrophages M0 and T cells follicular helper) were negatively related to the risk score (Fig. 7E). In addition, immunescore, stromalscore and estimatescore displayed lower in the low-risk subgroup (Fig. 8A). To conclude,

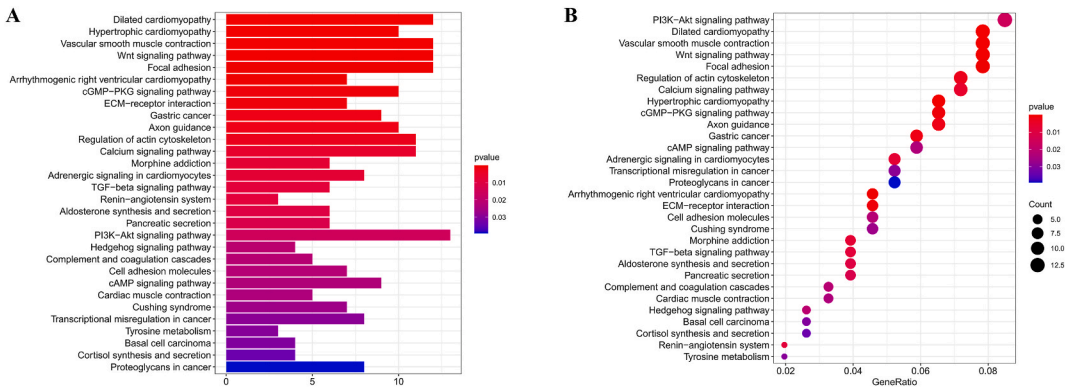

Fig. 6. GSEA analysis. (A–B) Signaling pathways enriched in our signature.

m5C-LPS could be able to distinguish different features of GC and might have a potential role in predicting immune response and guiding immunotherapy.

3.7. Clinical treatment and immunotherapy response

To investigate the therapy response of the two subgroups and provide more accurate treatment strategies. The TIDE algorithm was applied to estimate whether the risk signature could benefit from checkpoint inhibitors therapy. We found the TIDE score of low-risk subgroup displayed lower which indicated this subgroup less likely to develop immune escape and could benefit more from the immunotherapy (Fig. 8B). Drug sensitivity analysis based on the pRRophetic algorithm was utilized for seeking a possible cure. As depicted in the violin chart, the high-risk subgroup could benefit more from 35 antitumor drugs which showed the lower TIDE value, such as bryostatin, dasatinib, bexarotene, pazopanib, etc. (Fig. 8C, Supplementary Fig. S2). Furthermore, 5 antitumor drugs were identified to be extremely sensitive to the low-risk subgroup (Fig. 8D).

3.8. Expression level of 11 m5C-lncRNAs in GC cell lines

We next performed qRT-PCR to compare the expression of these lncRNAs in GES-1 and 3 GC cell lines (AGS, HGC-27, SGC-7901). As shown in Fig. 9, RHPN1-AS1, AC093752.3, AC048382.2, AC007405.2, AC036103.1, CCDC183-AS1, ADORA2A-AS1 were observed significantly upregulated in GC cell lines. Meanwhile, MAGI2-AS3 seemed to be lower in GC cells and TSC22D1-AS1, AL391152.1, AL033527.3 exhibited opposite tendency in different GC cell lines.

4. Discussion

In this study, we developed a gene signature of 11 m5C-lncRNAs using the TCGA GC population and validated its prognostic value in both train and test datasets. ROC curves demonstrated that the signature was superior to conventional clinical parameters. Additionally, the risk score was verified as an independent predictor of prognosis for GC via univariate and multivariate analysis. These results suggest that this signature could accurately predict the prognosis of GC. To apply this signature to clinical practice, we established a nomogram that can conveniently predict the prognosis of GC patients over 1, 3, and 5 years. Overall, this is the first m5C-LPS for GC, offering a promising path forward for diagnosis and treatment of this troubling malignancy.

Numerous long non-coding RNAs (lncRNAs) have been reported to be dysregulated in gastric cancer. For instance, HOTAIR functions as a competing endogenous RNA, regulating HER2 expression by sponging miR-331-3p in gastric cancer cells. Currently, RHPN1-AS1, MAGI2-AS3, CCDC183-AS1, and ADORA2A-AS1 have been reported among 11 m5C-related lncRNAs. In gastric cancer (GC), RHPN1-AS1 could enhance ETS1 expression via sponging miR-1299 to promote GC cell proliferation [30]. MAGI2-AS3, regulated by BRD4, can positively control ZEB1 expression, thereby promoting gastric cancer (GC) migration, invasion, and epithelial-mesenchymal transition (EMT) capabilities [31]. In hepatocellular carcinoma, CCDC183-AS1 could promote tumor progression, while ADORA2A-AS1 functions as a cancer suppressor [32,33].

The tumor microenvironment (TIME), encompassing various immune cells and secreted factors, plays a pivotal role in tumor genesis and development. Its heterogeneity can influence the prognosis and treatment response of cancer patients [34]. In our study, KEGG results indicated the signature might be correlated with cancer-related pathways while these ways were previously reported to be greatly associated with TIME. So we performed a series of analysis on immune cells infiltration. We found the estimatescores, immunescores and stromalscores of the high-risk subgroup seemed much higher which could represent a higher-degree of immune invasion and lower purity of tumor in the high-risk subgroup. Moreover, we discovered the high-risk subgroup present relatively higher levels of the following indicators, such as the amount of infiltrated immune cells, immune functions as well as immune checkpoints. A total of 15 immune checkpoints expressed at a higher level, which might be involved in mediating the immune escape and confer unfavorable prognosis for GC patients. Additionally, the risk score was found significantly associated with the infiltrated

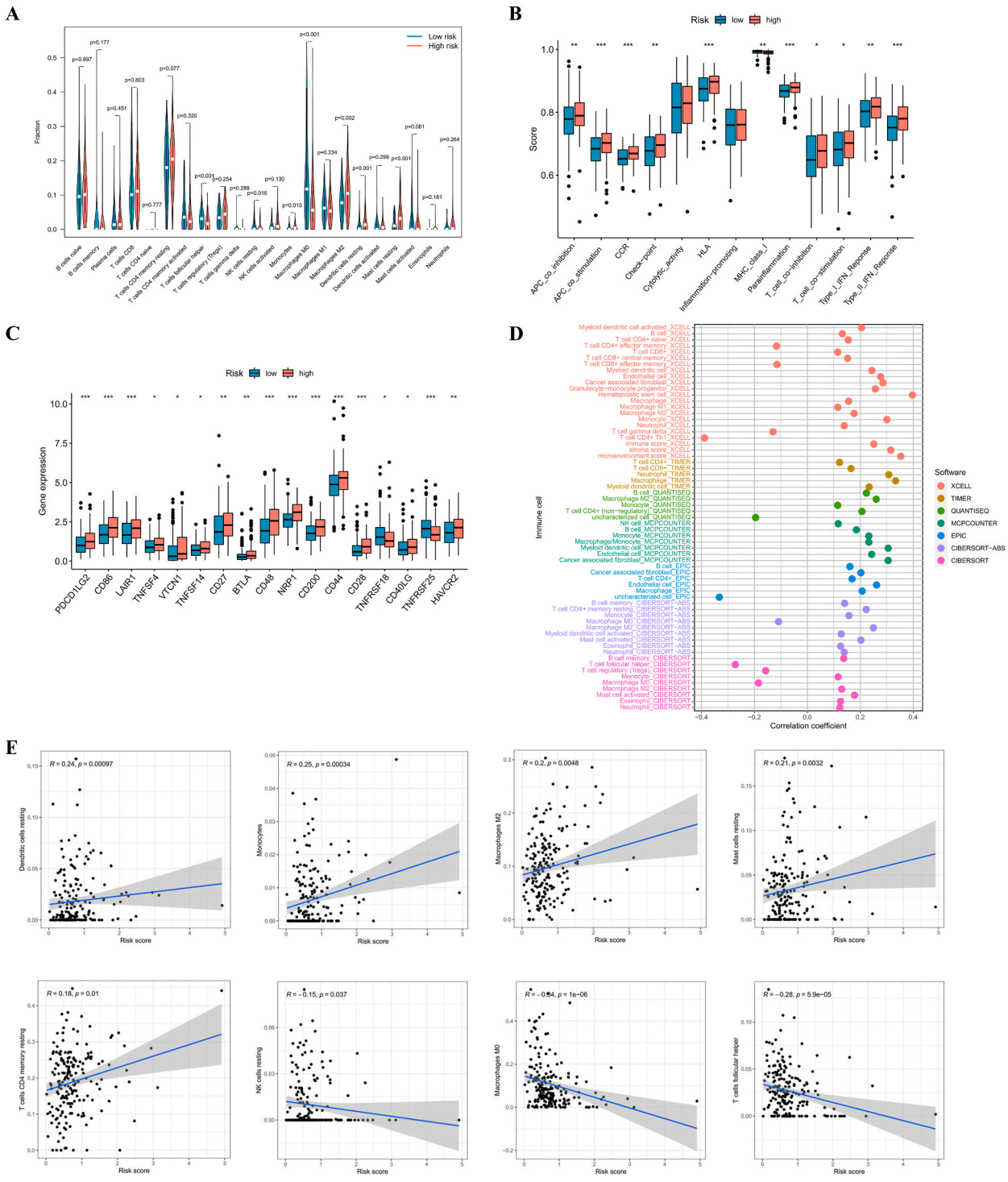

Fig. 7. Immune-related analysis. (A) The difference of 22 immune cells, (B) immune functions, (C) as well as 17 checkpoint inhibitors expression between the subgroups. (D) Bubble diagram plotted the correlation between risk score and immune cells based on 7 platform algorithms. (E) The correlation between risk score and infiltrated abundance of 7 immune cells based on CIBERSORT. $^{*}P < 0.05$, $^{**}P < 0.01$, $^{***}P < 0.001$.

abundance of immune cells. For example, the levels of Dendritic cells resting, Monocyte, Macrophage M2, Mast cells resting and T cells CD4 memory resting and the risk score revealed a positive correlation, moreover, the NK cells resting, Macrophage M0 and T cells follicular helper showed the opposite trend. And these correlation results were just in line with the previous immune cells differential expression results. Further, as the risk score increased, we could find that the infiltrated level of M2 macrophage increased which

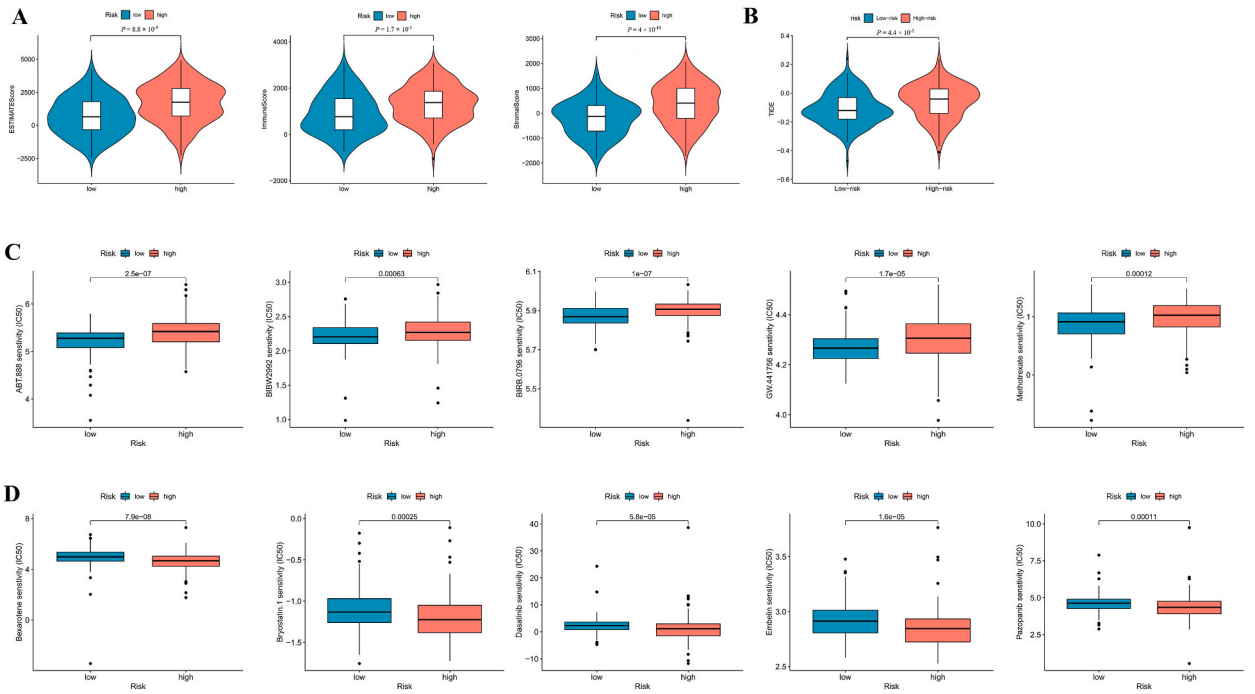

Fig. 8. The investigation of TME and drug sensitivity. (A) Comparisons of stromal and immune cells infiltrated levels, cancer purity, (B) immunotherapy response (C–D) and drug sensitivity analysis between the subgroups.

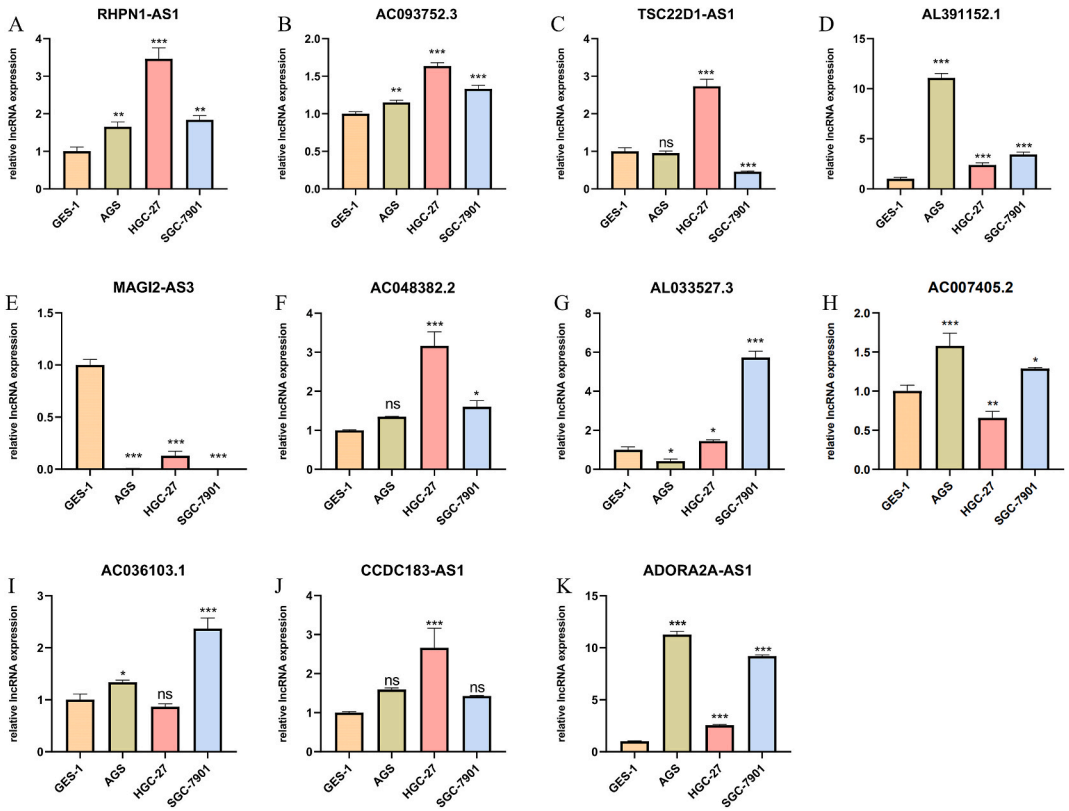

Fig. 9. The expression of 11 m5C-lncRNAs in GES-1 and 3 GC cell lines.

suggested that M2 macrophage may significantly act in the poor OS outcomes of the high-risk subgroup. A previous study revealed M2 macrophages could make extremely effects in human cancers by producing growth-promoting molecules to stimulate tumor development [35,36]. Furthermore, monocytes can exhibit antitumor functions or give rise to activated antigen-presenting cells. This dual effect depends on their response to the tumor microenvironment (TME) [37]. T follicular helper cells, which encompass numerous subsets, may also execute the same two functions by secreting a variety of different chemokines [38]. All the aforementioned results may elucidate why the high-risk subgroup exhibits diminished responsiveness to immunotherapy and has a propensity for immune evasion. Furthermore, not only immune checkpoints but also tumor mutation load, as well as microsatellite instability-high status, are strongly associated with the efficacy of immunotherapy [39]. Taken together, our study suggests that the m5C-LPS could be significantly valuable in predicting prognosis, reshaping the TIME and providing hopeful insights for effective clinical immunotherapy of GC patients.

However, our study has several limitations. Firstly, the initial data used for constructing the signature were solely obtained from TCGA, resulting in a relatively small sample size. Consequently, the signature was only validated through internal verification, without external database validation. Secondly, further basic experiments are necessary to confirm the content of m5C-lncRNAs. Lastly, additional research is required to elucidate the role of m5C-LPS in gastric cancer (GC), which could inform potential strategies for modulating the tumor immune microenvironment (TIME) and offer precision immunotherapy for GC.

5. Conclusion

To conclude, we systematically analyzed the expression of m5C-lncRNAs in gastric cancer (GC), developed an 11 m5C-LPS, and explored its prognostic value and potential functions on the tumor microenvironment (TIME). All analyses showed that the prognostic signature could act as an independent prognostic predictor and might be a crucial mediator in the TIME of GC. This finding may provide a promising therapeutic target for improving the immunotherapy effect of GC. Our findings may provide potential biomarkers or treatment targets, and provide a theoretical foundation for future basic research on m5C-lncRNAs for GC.

Funding

No Funding.

Declarations of consent for publication

Not applicable.

Ethics approval and consent to participate

(Not applicable) TCGA and GSEA are publicly accessible databases. Patient data are ethically approved. Data can be downloaded and used for research and publication. We used open-source data, so there are no ethical concerns or conflicts of interest. We declare that all methods and protocols were carried out by the relevant guidelines and regulations.

CRediT authorship contribution statement

Qingyu Song: Writing – review & editing, Writing – original draft, Supervision, Software. **Jingyu Wu:** Formal analysis, Data curation. **Hao Wan:** Methodology, Investigation. **Desen Fan:** Software, Resources, Funding acquisition.

Declaration of competing interest

The authors declare that they have no known competing financial interests or personal relationships that could have appeared to influence the work reported in this paper.

Acknowledgements

All authors appreciate TCGA, GENECODE database for sharing the original data.

Appendix A. Supplementary data

Supplementary data to this article can be found online at https://doi.org/10.1016/j.heliyon.2024.e37290.

References

[1] H. Sung, et al., Global cancer statistics 2020: GLOBOCAN estimates of incidence and mortality worldwide for 36 cancers in 185 countries, CA Cancer J Clin 71 (3) (2021) 209–249.
[2] A.P. Thrift, H.B. El-Serag, Burden of gastric cancer, Clin. Gastroenterol. Hepatol. 18 (3) (2020) 534–542.
[3] M.H. Shahrajabian, W. Sun, Survey on multi-omics, and multi-omics data analysis, integration and application, Curr. Pharmaceut. Anal. 19 (2023) 267–281.
[4] I.A. Roundtree, et al., Dynamic RNA modifications in gene expression regulation, Cell 169 (7) (2017) 1187–1200.
[5] Q. Zhang, et al., The role of RNA m(5)C modification in cancer metastasis, Int. J. Biol. Sci. 17 (13) (2021) 3369–3380.
[6] K. Liu, et al., Comparison between gastric and esophageal classification system among adenocarcinomas of esophagogastric junction according to AJCC 8th edition: a retrospective observational study from two high-volume institutions in China, Gastric Cancer 22 (3) (2019) 506–517.
[7] T. Jin, et al., Effectiveness and safety of robotic gastrectomy versus laparoscopic gastrectomy for gastric cancer: a meta-analysis of 12,401 gastric cancer patients, Updates Surg (2021).
[8] L. Mei, et al., RNA methyltransferase NSUN2 promotes gastric cancer cell proliferation by repressing p57(Kip2) by an m(5)C-dependent manner, Cell Death Dis. 11 (4) (2020) 270.
[9] X. Dai, et al., YTHDF2 binds to 5-methylcytosine in RNA and modulates the maturation of ribosomal RNA, Anal. Chem. 92 (1) (2020) 1346–1354.
[10] A. Bhan, M. Soleimani, S.S. Mandal, Long noncoding RNA and cancer: a new paradigm, Cancer Res. 77 (15) (2017) 3965–3981.
[11] S.J. Liu, et al., Long noncoding RNAs in cancer metastasis, Nat. Rev. Cancer 21 (7) (2021) 446–460.
[12] L. Chen, et al., The Role of non-coding RNAs in colorectal cancer, with a focus on its autophagy, Pharmacol. Ther. 226 (2021) 107868.
[13] E.M. McCabe, T.P. Rasmussen, lncRNA involvement in cancer stem cell function and epithelial-mesenchymal transitions, Semin. Cancer Biol. 75 (2021) 38–48.
[14] Z. Sun, et al., Aberrant NSUN2-mediated m(5)C modification of H19 lncRNA is associated with poor differentiation of hepatocellular carcinoma, Oncogene 39 (45) (2020) 6906–6919.
[15] Y. Wang, et al., LncRNA LINRIS stabilizes IGF2BP2 and promotes the aerobic glycolysis in colorectal cancer, Mol. Cancer 18 (1) (2019) 174.
[16] J. Pan, Z. Huang, Y. Xu, m5C RNA methylation regulators predict prognosis and regulate the immune microenvironment in lung squamous cell carcinoma, Front. Oncol. 11 (2021) 657466.
[17] K. Wang, et al., 5-Methylcytosine RNA methyltransferases-related long non-coding RNA to develop and validate biochemical recurrence signature in prostate cancer, Front. Mol. Biosci. 8 (2021) 775304.
[18] Z. Huang, et al., Prognostic significance and tumor immune microenvironment heterogenicity of m5C RNA methylation regulators in triple-negative breast cancer, Front. Cell Dev. Biol. 9 (2021) 657547.
[19] B. Lu, et al., Basic transcription factor 3 like 4 enhances malignant phenotypes through modulating tumor cell function and immune microenvironment in glioma, Am. J. Pathol. 194 (5) (2024) 772–784.
[20] L. Bejarano, M.J.C. Jordao, J.A. Joyce, Therapeutic targeting of the tumor microenvironment, Cancer Discov. 11 (4) (2021) 933–959.
[21] H. Sadeghi Rad, et al., Understanding the tumor microenvironment for effective immunotherapy, Med. Res. Rev. 41 (3) (2021) 1474–1498.
[22] K. Liu, et al., The value of spleen-preserving lymphadenectomy in total gastrectomy for gastric and esophagogastric junctional adenocarcinomas: a long-term retrospective propensity score match study from a high-volume institution in China, Surgery 169 (2) (2021) 426–435.
[23] C. Weng, et al., Identification of a N6-methyladenosine (m6A)-Related lncRNA signature for predicting the prognosis and immune landscape of lung squamous cell carcinoma, Front. Oncol. 11 (2021) 763027.
[24] Z. Zhao, et al., Necroptosis-related lncRNAs: predicting prognosis and the distinction between the cold and hot tumors in gastric cancer, J Oncol 2021 (2021) 6718443.
[25] Q. Geng, et al., Comprehensive analysis of the prognostic value and immune infiltrates of the three-m5C signature in colon carcinoma, Cancer Manag. Res. 13 (2021) 7989–8002.
[26] M. Huang, et al., m5C-Related signatures for predicting prognosis in cutaneous melanoma with machine learning, J Oncol 2021 (2021) 6173206.
[27] H. Yuan, et al., Prognostic risk model and tumor immune environment modulation of m5C-related LncRNAs in pancreatic ductal adenocarcinoma, Front. Immunol. 12 (2021) 800268.
[28] S.G. Pai, et al., Wnt/beta-catenin pathway: modulating anticancer immune response, J. Hematol. Oncol. 10 (1) (2017) 101.
[29] B. Vanhaesebroeck, et al., PI3K inhibitors are finally coming of age, Nat. Rev. Drug Discov. 20 (10) (2021) 741–769.
[30] L. Ding, et al., The positive feedback loop of RHPN1-AS1/miR-1299/ETS1 accelerates the deterioration of gastric cancer, Biomed. Pharmacother. 124 (2020) 109848.
[31] D. Li, et al., LncRNA MAGI2-AS3 is regulated by BRD4 and promotes gastric cancer progression via maintaining ZEB1 overexpression by sponging miR-141/200a, Mol. Ther. Nucleic Acids 19 (2020) 109–123.
[32] H. Zhu, et al., Long non-coding RNA CCDC183-AS1 acts AS a miR-589-5p sponge to promote the progression of hepatocellular carcinoma through regulating SKP1 expression, J. Exp. Clin. Cancer Res. 40 (1) (2021) 57.
[33] J. Pu, et al., ADORA2A-AS1 restricts hepatocellular carcinoma progression via binding HuR and repressing FSCN1/AKT Axis, Front. Oncol. 11 (2021) 754835.
[34] D.C. Hinshaw, L.A. Shevde, The tumor microenvironment innately modulates cancer progression, Cancer Res. 79 (18) (2019) 4557–4566.
[35] C.D. Mills, L.L. Lenz, R.A. Harris, A breakthrough: macrophage-directed cancer immunotherapy, Cancer Res. 76 (3) (2016) 513–516.
[36] J. Lan, et al., M2 macrophage-derived exosomes promote cell migration and invasion in colon cancer, Cancer Res. 79 (1) (2019) 146–158.
[37] S. Ugel, et al., Monocytes in the tumor microenvironment, Annu. Rev. Pathol. 16 (2021) 93–122.
[38] J.M. Pitt, et al., Targeting the tumor microenvironment: removing obstruction to anticancer immune responses and immunotherapy, Ann. Oncol. 27 (8) (2016) 1482–1492.
[39] Y. Baba, et al., Tumor immune microenvironment and immune checkpoint inhibitors in esophageal squamous cell carcinoma, Cancer Sci. 111 (9) (2020) 3132–3141.